Chapter 11
Understanding Changes in Global Behavior Due to Control Location

Sarah Johnson, John Schultze, and Shannon Danforth

Abstract In distributed shaker, multi-axis testing, any number of locations and degrees of freedom can be used as control channels. Using differing control degrees of freedom can affect the global behavior of the test article, changing the response from the field. This study aims to examine how the response at monitored locations changes due to moving the controlled degrees of freedom on a test article. Initially, the control degrees of freedom are collocated with the drive point of a distributed shaker. Then, they are moved to a more compliant part of the test article, away from the actuator. To assess the quality of each test, the response at several monitored points will be compared to the field response using a multi-tiered approach. Understanding how control degrees of freedom affect the global behavior of the test article can help test engineers make more informed decisions about where to control and how to determine the quality of a test.

Keywords Multi-axis · Metrics · Aggregate ASD · MIMO · PSDPM

Introduction

Multi-axis vibration testing consists of exciting a structure in several directions simultaneously, as opposed to traditional single-axis testing which involves sequential tests in each principal axis of the test article. Multi-axis loading can be more representative of in-service environments because it allows greater flexibility in approximating boundary conditions. It also better approximates complex loading which can make the test environment more similar to the field environment. There are several methods to perform multi-axis vibration testing, and several methods for analyzing multi-axis vibration data.

Distributed shaker methods such as impedance matched multi-axis testing (IMMAT) involve attaching several shakers across the body of the test article and imparting force via a stinger [1]. Distributed shaker methods have largely been considered for flight environments where the test article experiences distributed loading across its surface. Previous researchers have had success matching flight relevant vibration levels using many control locations [2]. However, when any location on the test article can be a candidate shaker location, the design space of the test becomes quite large. It is also difficult to impart large forces and displacements using distributed shakers. There is no standard to define what is "good enough" in these styles of testing, primarily due to a lack of data from field testing. In addition, it can be difficult to assess the large amounts of data from these tests and determine how much better a multi-axis test approximated the field condition, especially when it comes to monitored locations that were not used for control.

In addition to distributed shaker methods, base-excited multi-axis vibration testing methods have also gained popularity. In a base-excited vibration test, the test article is rigidly attached to some sort of platform with a fixture, and the platform is excited in such a way that replicates the field environment. Bolting the test article to a shaker table with a rigid fixture, much like traditional single-axis testing techniques, reduces the complexity of the test set up and design. Base-excited methods can be used for transportation environments, where test articles are fixed to a platform and experience loading from the connection surface, a boundary condition that can be more readily replicated in a lab setting. Researchers have had success with commercial 6 degree-of-freedom shaker tables, custom-designed shaker platforms that have been used for component level testing, and and custom-designed shaker tables [3] [4].

Assessment of multi-axis testing can also be challenging. Due to the large number of control degrees of freedom and monitored degrees of freedom, it can be difficult to resolve what is a successful test. Kramer et al. used several metrics to try and assess how well multi-axis testing compares to single-axis testing [5], but the results are often limited to comparing one or

Sarah Johnson · John Schultze · Shannon Danforth
Los Alamos National Laboratory, Los Alamos, NM 87545
e-mail: sarahmjohnson2018@gmail.com; schultze@lanl.gov; sdanforth@lanl.gov

Alexandra Karlicek et al. (eds.), *Dynamic Environments Testing, Vol. 7*, Conference Proceedings
of the Society for Experimental Mechanics Series, https://doi.org/10.13052/97887-438-0152-8_11

two control degrees of freedom at a time. Rohe et al. used an aggregate technique that adds all controlled autopower spectral density (ASD) responses and compares them to the sum of all control specifications [2]. Adding ASDs together results in much less data to compare but loses the information about how each channel responds. Also, there is no exploration of how the loss in resolution might affect the overall assessment of the test.

There are many difficulties with multi-axis testing, from implementation to assessment. This study aims to explore how changing the control location on a test article changes the response at monitored locations on the test article while utilizing a multi-axis test approach. In addition, this study will focus on data presentation can affect a test engineer's ability to quickly and accurately determine if a test was successful. We will assess the G_{RMS}, dB error (e_{dB}), and the frequency response function similarity metric (FRFSM) on aggregate response as well as individual response to determine what "level" of fidelity is needed in analysis to assess the global behavior of the system compared to what it sees in the field.

Testing

Field test

In this study, the Generic OBject for Laboratory Environmental Testing (GOBLET) is used as the test article. The GOBLET is an aluminum, three-piece assembly that is used to assess complex dynamics of cylindrical components. The GOBLET's three parts are an adapter plate, a cylindrical mass, and a bell, which are shown in Figure 1. The bell is thin-walled and is relatively compliant, especially when attached to the more rigid cylinder. The bell bolts onto the cylinder at 3 legs. The GOBLET adapter plate and cylinder primarily exhibit rigid body motion, with their axial motion being nearly identical to the input at the base of the assembly.

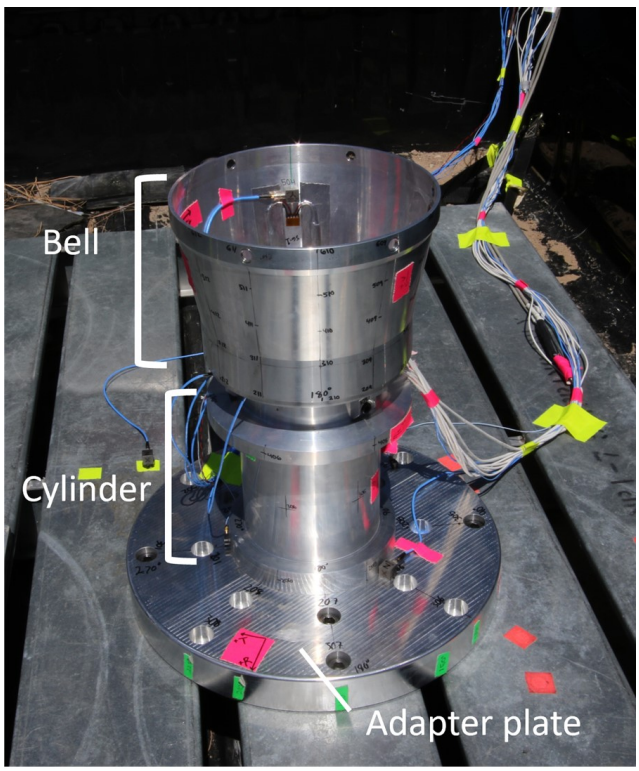

Fig. 1 Configuration of GOBLET during field testing.

To have a set of reference data, we field tested the GOBLET in a transportation environment. To perform this testing, six tri-axial accelerometers and three uni-axial accelerometers were attached across the GOBLET assembly. The bell piece had four tri-axial accelerometers, with two on one of the legs and two at different heights along the bell. The assembly was bolted to a metal pallet that secured in the bed of a truck, as shown in Figure 1. We then drove the truck around several paved and dirt roads to record different types of excitation at many levels.

To use the data from the field as an environmental test specification, we examined the time data and found a segment that had high levels of random vibration and did not contain shocks. Then, we computed a coarse ASD of the segment and used it as a comparison state between the different environmental tests. At frequencies above 500 Hz, the ASDs exhibited energy levels that were below the noise floor of the accelerometers used, so the high frequency data was excluded from analysis. Below 30 Hz, the ASDs exhibited displacement levels that were too high for the modal shaker used in this study. When creating specifications, we considered a truncated frequency range of 30 to 515 Hz.

Environmental test

To recreate the field condition in the lab, we used a technique involving a large, single-axis shaker and a distributed, modal shaker. The base excitation was provided by a Unholz-Dickie (UD) H560 single-axis shaker on which the test assembly was bolted. The placement and securing of the GOBLET on the single-axis shaker mirrors the boundary condition that the GOBLET experienced in the field closely. In addition to the base excitation, we also placed a distributed shaker, from here forward referred to as the *supplemental shaker*, on the test article. The location for the supplemental shaker was chosen based on lessons learned from prior testing, namely that the stinger drive block was most likely to stay attached to the cylinder due to its rigidity as opposed to the bell. The supplemental shaker was a 100-pound-force shaker from The Modal Shop with model number 2100E11. Excitation was imparted by a metal stinger which threaded into a custom drive block that was secured to the assembly using dental cement. The test set up is shown in Figure 2. Further information about this testing technique can be found in [6].

During the laboratory testing, two degrees of freedom (DOFs) were used as control channels. In the first set of tests, the control DOFs were located at the supplemental shaker drive point (see Figure 3(a)). The tests were controlled axially and radially by the UD shaker and the supplemental shaker, respectively. In the second set of test runs, the control DOFs were placed at a location 90 degrees from the drive location on the bell which is a more compliant region of the GOBLET

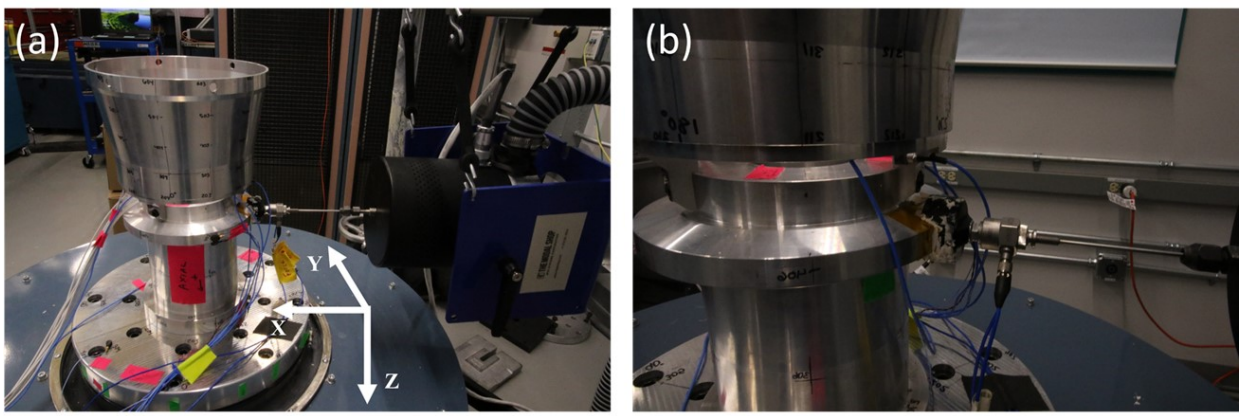

Fig. 2 GOBLET during laboratory testing with (a) full configuration and coordinate system and (b) drive block attachment.

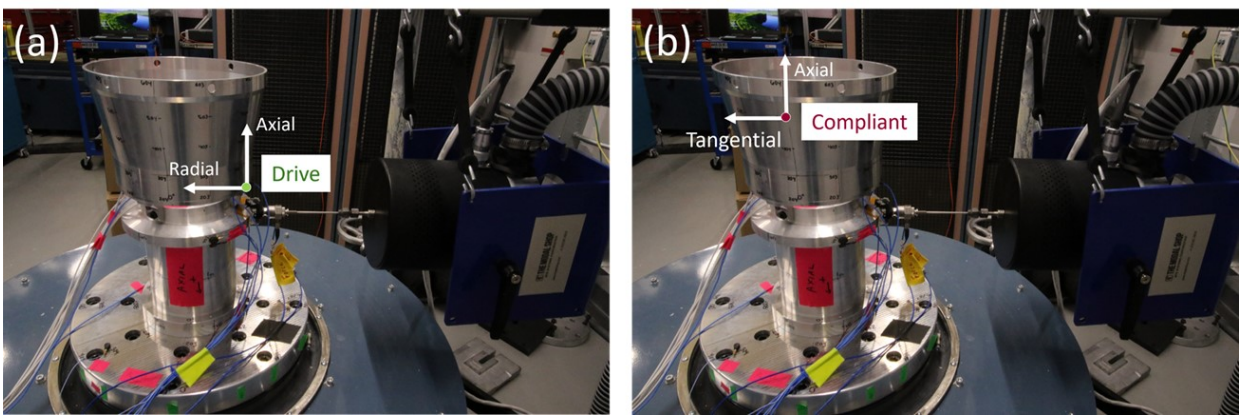

Fig. 3 Control degrees of freedom for (a) drive point control and (b) control from compliant location.

(see Figure 3(b)). One DOF was excited axially by the UD shaker, and the other DOF was excited tangentially by the supplemental shaker. It is important to note that the supplemental shaker was in the same location for both sets of tests.

Analysis

The goal of this analysis is to investigate what level of analysis allows us to detect which set of control DOFs results in the "best" test. For this case study, the best control location of the two will be determined by applying a series of metrics and assessing which is closest to the field response (explained further in next section). At the first level, we will take the sum of the ASDs of all channels and make comparisons between the field test and the global behavior based on the aggregate ASD. To compute the aggregate ASD, we will use the sum of autopower spectral densities used in [2] which will provide a single ASD curve consisting of the sum of the 21 channels present in the test. There will be one curve for the field response, one from the drive environmental test, and one from the compliant environmental test. When calculating the average ASD, we will only consider the DOFs that were present in both the field test and the laboratory test. The sensors corresponding to these DOFs were not moved or modified from the field configuration.

At the second level, we will assess the ASDs by direction. We will look at the sum of all X-direction ASDs, then Y-direction ASDs, and then Z-direction ASDs. Finally, at the third level, we will examine individual monitored location ASDs. For the sake of brevity, we will only examine the responses from one tri-axial accelerometer in this paper.

Our motivation for the tiered approach is to determine if a coarse analysis can provide a similar assessment of test performance when compared to a more detailed approach. The aggregate ASD analysis is a common strategy when test engineers need a quick assessment of a test, especially in situ. Through this study, we can improve confidence in this assessment technique as well as assess how different error metrics can affect the perceived performance.

Error metrics

One of the most common ways that vibration tests are assessed is using the G_{RMS}. The G_{RMS} of a autopower spectral density (ASD) curve represents the average energy across a frequency range and corresponds to the area under the ASD curve. The G_{RMS} is computed as

$$G_{RMS} = \frac{1}{n_{freq}} \sqrt{\sum_{i=1}^{n_{freq}} G_{xx}(f_i)^2}, \tag{1}$$

where $G_{xx}(f_i)$ is the auto spectral density value at the i^{th} frequency line, for $i \in \{1, 2, ..., n_{freq}\}$. The G_{RMS} is often used because it simplifies the ASD to a single value, thus making test results easier to understand. However, it is sensitive to large amplitude response. This sensitivity can cause high amplitude excursions to appear much more severe than low amplitude excursions or under tests, resulting in an unreliable value.

Another common assessment of how well a test controlled is the decibel (dB) error. The dB error involves determining the dB difference between a response and some sort of reference. The mean dB error is given by

$$e_{dB}(f_i) = \frac{1}{n_{freq}} \sum_{i=1}^{n_{freq}} 10 \log \left(\frac{G_{xx}(f_i)}{G_{ref}(f_i)} \right), \tag{2}$$

where G_{xx} is the response ASD at the i^{th} frequency line and G_{ref} is the specification ASD at the i^{th} frequency line. Because the dB calculation involves a ratio of response to reference, dB error is equally sensitive to large amplitude excursions as it is to low amplitude excursions. We are interested in the total energy in the system for comparison, so we will be using the dB error instead of the RMS dB error or absolute dB error, which is another common test assessment.

Finally, we use a metric called the frequency response function similarity metric (FRFSM). While this method was originally developed to assess the differences in FRFs between analytical models and experiments by [7], the FRFSM can be used to compare any two signals at its basic level. Because we will be comparing ASD signals instead of FRFs, we will call this metric the power spectral density probability metric (PSDPM) for clarity. At each frequency line i (for $i \in \{1, 2, ..., n_{freq}\}$), a probability density function (PDF) $g(x_i, \mu_i, \sigma_i^2)$ is created:

$$g(x_i, \mu_i, \sigma_i^2) = \left(\frac{1}{\sigma_i \sqrt{2\pi}} \right) exp \left(-\frac{1}{2} \left(\frac{x_i - \mu_i}{\sigma_i} \right)^2 \right). \tag{3}$$

where the PDF is centered at a mean value μ_i with distribution width σ_i, and an error metric value of x_i. We will be using the dB error described in Equation 2 as the x_i value. The mean value of the PDF is set to zero, indicating perfect agreement between the response and specification, and the distribution is set such that 3σ on the PDF is equivalent to 6 dB, which is a common abort limit in environmental testing. The PSDPM value is then normalized by a PDF with a mean and error metric value of 0 to ensure the final value will be between 0 and 1:

$$\text{PSDPM} = \frac{1}{n_{freq}} \sum_{i=1}^{n_{freq}} \frac{g(e_{dBi}, 0, \sigma_i^2)}{g(0, 0, \sigma_i^2)} \tag{4}$$

where we will be computing the PSDPM at each frequency line then using the RMS value for assessment. The PSDPM offers a different perspective into the error between field and environmental response. At each frequency line, the PSDPM gives the probability that the dB error between the field and environmental response is zero, that is that the responses are the same. For comparison to other scalar-value metrics in this paper, we compute the RMS of the PSDPM across frequency lines. We consider this PSDPM RMS as an alternative measure of how well the specification/field environment was achieved by a given test.

Difference in response

Before we can make an assessment of how similar the global response of the GOBLET was between the lab and the field, we must first ensure that the control DOFs were controlled well in the environmental test. To assess this, we will first use visual inspection, then apply the error metrics from the previous section. In Figure 4, we see agreement when controlling to

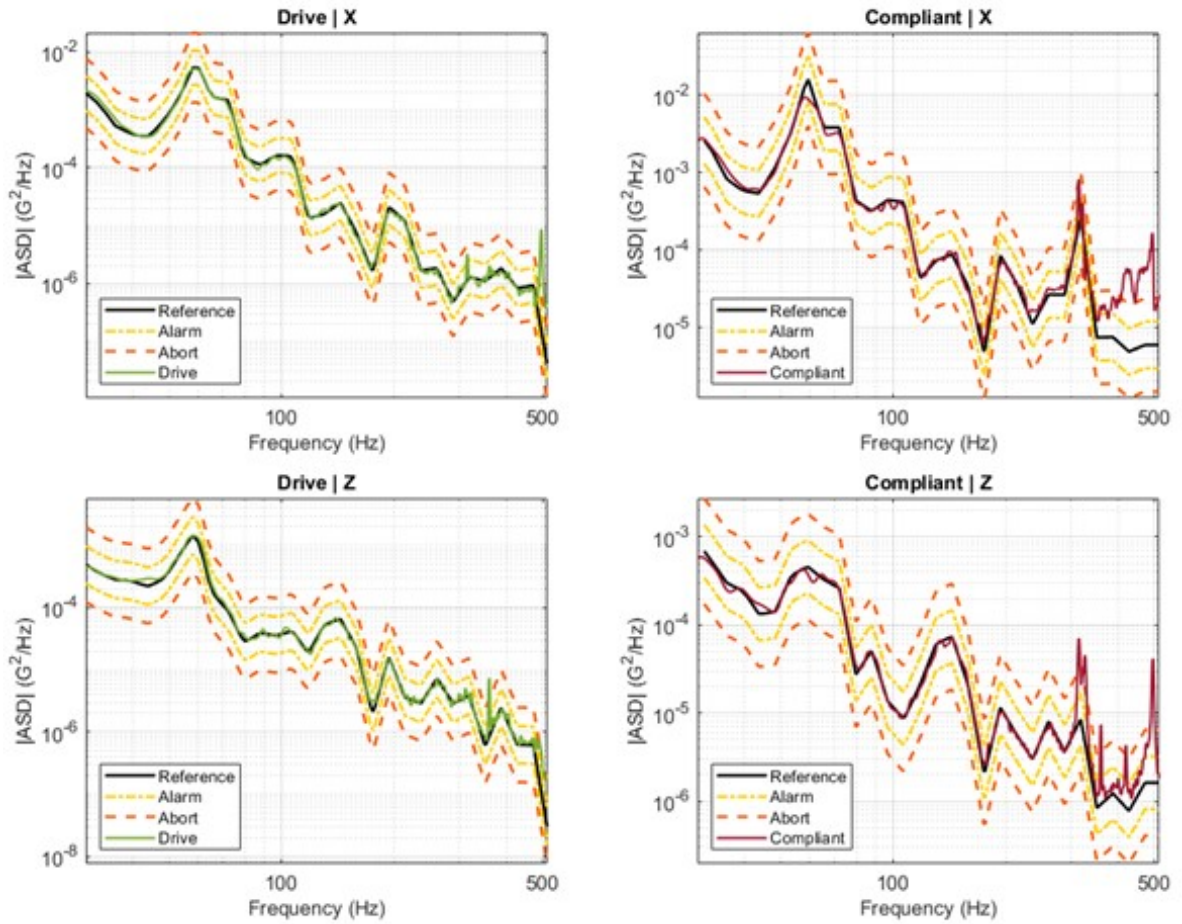

Fig. 4 Response at controlled DOFs compared to reference specifications derived from field data with ± 3 dB alarm limits and ± 6 dB abort limits.

the drive DOFs for the entire frequency range. When we look at numerical assessment of the control DOFs independently of the figure in 1, we can see that based on G_{RMS} alone, the compliant control appears the perform better, but when comparing the dB error and PSDPM, we see that the drive control error values were lower. This assessment is in alignment with the visual inspection of the control ASD which confirms that much of the response was outside the alarm and abort lines after 300 Hz in the compliant control which can be seen in 4. This excursion is not reflected in the G_{RMS} values but is reflected in the e_{dB} and PSDPM. The excursion above 300 Hz could be due to the low amplitude level of the specification, or simply that the controller was not able to match the specification in that region, especially in the Y direction. Already we can see that the controlling at the drive location was more achievable for the controller, however in further sections we will explore how the control affects the other responses in the system.

Table 1 Control Channel Error Metrics

Control Channel Error Metrics				
Configuration	**DOF**	**G_{RMS}**	**dB Error**	**PSDPM**
Reference Drive	X	0.291	0.0	1.0
	Z	0.155	0.0	1.0
Drive	X	0.283	0.508	0.925
	Z	0.157	0.678	0.921
Reference Compliant	X	0.439	0.0	1.0
	Z	0.134	0.0	1.0
Compliant	X	0.417	11.6	0.137
	Z	0.134	2.650	0.695

Next, we will examine the results using metrics of different fidelity levels to determine if we can tell which control DOFs resulted in a better matched global response to the field data and at what fidelity in response we are able to arrive at this conclusion.

Total ASD

At the highest level, we consider the sum of the 21 channels in the field test compared to the sum of the channels in the laboratory test. Before assessment, the G_{RMS} was used to perform a statistical t-test at 90% confidence to ensure there was a statistical difference between the field response and the environmental test responses. The t-test showed that there was a significant difference in the global response. In Figure 5, we see that for both the compliant and drive control configurations,

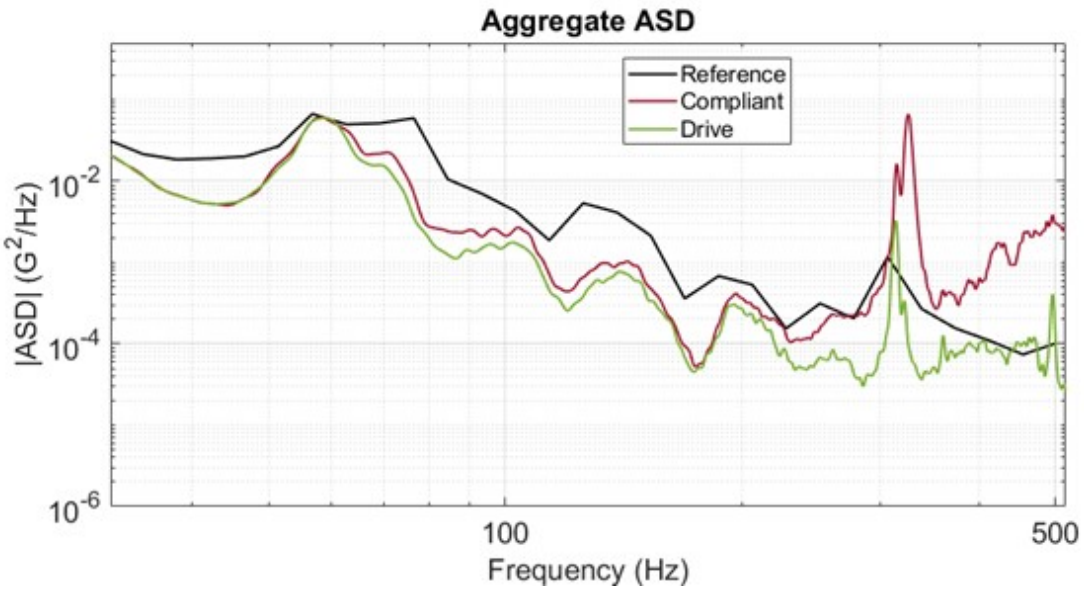

Fig. 5 The sum of all ASDs from the field test (reference), the drive control configuration, the compliant control configuration.

the response appears below the field response for most of the frequency range. However, after a large excursion at 350 Hz, the compliant control configuration has more energy than the field reference. This region is the same one where we noted that the controller was not able to match the specification, shown in Figure 4, which could be the reason for the excess energy in the aggregate ASD.

In Table 2, we can see that compliant configuration resulted in a G_{RMS} closer to that of the reference. We notice high dB error for the drive DOFs but a better PSDPM than the compliant control. Overall at this stage of assessment, it is difficult to tell which control DOFs performed closer to the field reference.

Table 2 Error Metrics for aggregate ASD response

Aggregate ASD Error Metrics			
Configuration	**G_{RMS}**	**dB Error**	**PSDPM**
Reference	1.562	0.0	1.0
Drive	0.987	-4.857	0.430
Compliant	1.390	1.930	0.387

X, Y, Z ASD

Next, we will assess how the control DOFs affected the total response in the principal axes of the system, X, Y, and Z. Note that there were several sensors that were not placed on the principal axes, and these channels were projected onto the principal axes using transformation matrices. In Figure 6, we see that the combined responses in the X-direction appear to follow the field reference well. However, the drive configuration is just below the specification for the entire frequency range of interest while the compliant direction follows the reference much more closely. Both configurations show a high response near 320Hz. In the Y-direction, the response do not match the specification well, most likely because there were no control DOFs in the Y-axis. In the Z-direction, both configurations appear to follow a somewhat similar profile of the specification but at a lower magnitude until near 320 Hz. This result is surprising because the Z-direction corresponds to up and down

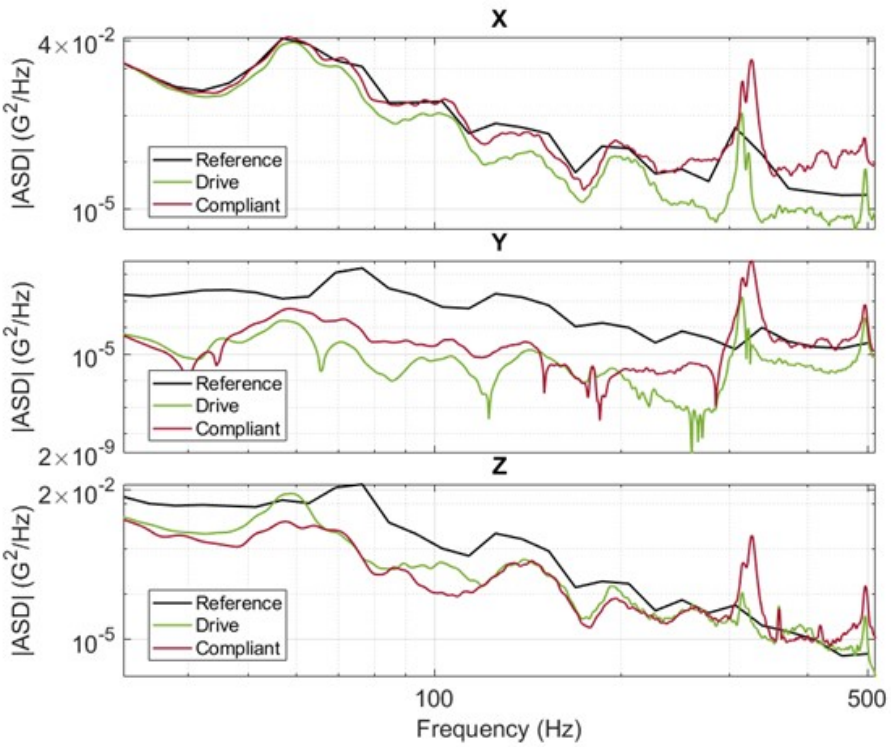

Fig. 6 The sum of the X, Y, and Z direction ASDs from the field test (Reference), the drive control configuration, and the compliant control configuration.

movement of the truck bed which was found to be mostly rigid through the assembly. As such, we would expect that having control channels in that direction would result in a combined response more similar to the field.

Numerically, we see that the drive location has a larger magnitude dB error in all directions compared to the compliant control. In addition, the PSDPM for the compliant control was higher in the X-direction, indicating that it was better agreement with the reference. However, the Z-direction PSDPM was slightly higher for the drive configuration than the compliant.

Table 3 Error metrics for combined X, Y, and Z ASD Response

Control Channel Error Metrics				
Configuration	**DOF**	**G_{RMS}**	**dB Error**	**PSDPM**
Reference	X	0.948	0.0	1.0
	Y	0.628	0.0	1.0
	Z	0.913	0.0	1.0
Drive	X	0.756	-5.657	0.304
	Y	0.112	-15.00	0.180
	Z	0.518	-2.50	0.582
Compliant	X	0.985	2.314	0.609
	Y	0.535	-6.791	0.394
	Z	0.394	-1.746	0.472

Individual channels

Finally, we will look at single response channel to assess the global response of the system. In an environmental test, looking at each monitored, response accelerometer could be quite time consuming and would be considered a last resort as an assessment of a test's quality. However, we must check that individual responses agree with conclusions that we may draw from the previous, coarse analyses, so we can access the reliability of the summed ASDs.

We will assess the individual accelerometer response at location 1504. Location 1504 is on the top surface of the cylinder of the GOBLET, at approximately 180 degrees from the drive location and 90 degrees from the compliant location as shown in Figure 7. This location was chosen because it is not on the same part of the assembly as the control DOFs for either configuration. Therefore, location 1504 is representative of a common practice in environmental testing where it is assumed

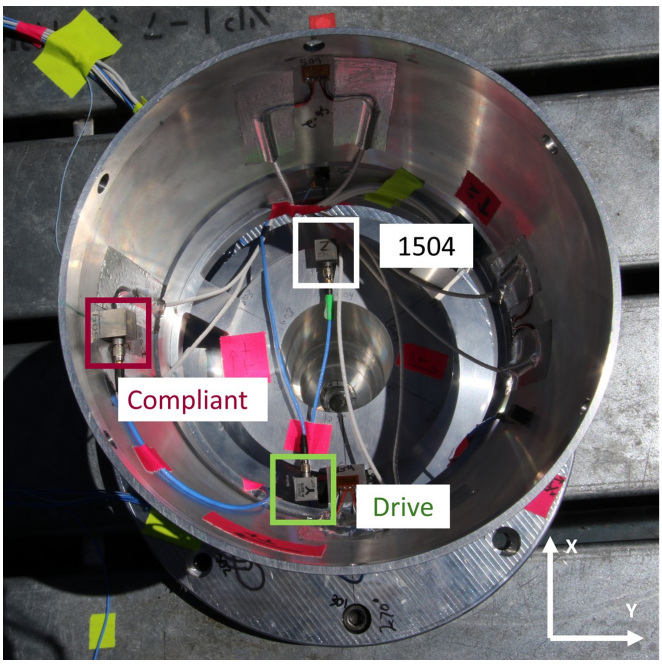

Fig. 7 Location 1504 with respect to the drive and compliant locations.

that controlling an assembly at one location results in a response similar to the field environment across portions of the assembly that are in proximity to the controlled DOFs.

The X DOF appears to follow the field response well, especially in the drive configuration. The compliant configuration follows the field response profile well until about 250 Hz which is near where the controller was not performing well. The Y DOF is much lower than the field response, which was expected as there was no control DOF in that direction. The Z direction, which had a control DOF, appears to not follow the field response as closely as the X direction, but has a similar profile and results in a slight over test of the the 1504 location. These results appear consistent with the total response and the principal axes response.

Assessing the error metrics in 4, we can similar difference in the G_{RMS} in both the configurations. We see low dB error for the Z-direction response for both configurations. The PSDPM for the drive configuration is much higher than the compliant configuration in the X-direction but is similar, if not lower, in the Y and Z-directions.

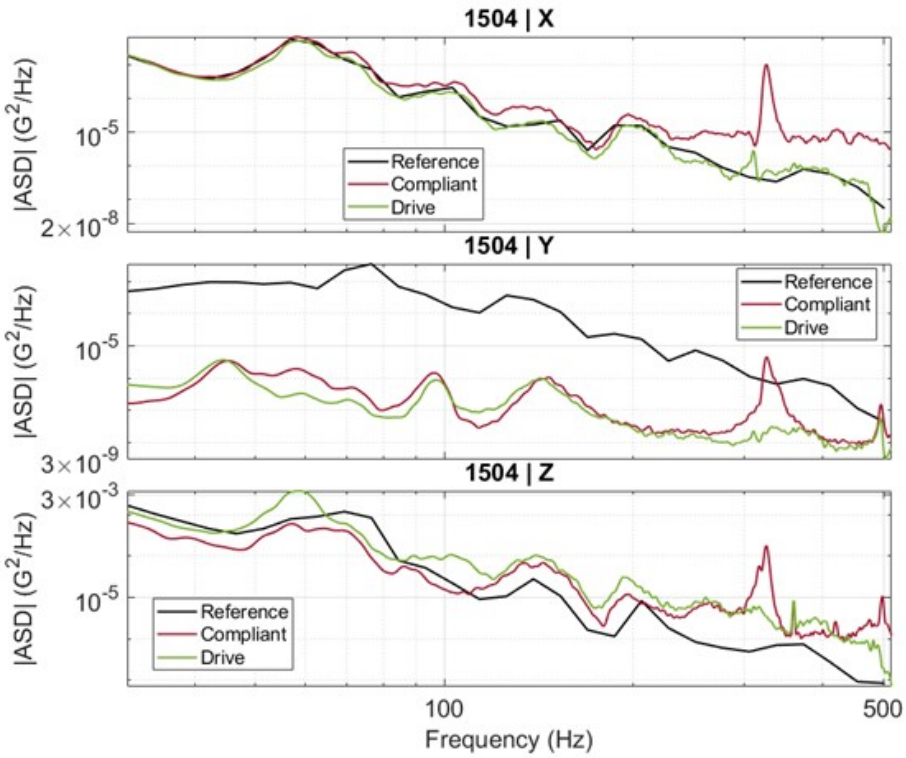

Fig. 8 Response of single accelerometer placed on cylinder portion of the assembly from the field (reference), the drive control configuration, and the compliant control configuration.

Table 4 Error Metrics for Response at Location 1504

Control Channel Error Metrics				
Configuration	**DOF**	**G_{RMS}**	**dB Error**	**PSDPM**
Reference	X	0.314	0.0	1.0
	Y	0.306	0.0	1.0
	Z	0.314	0.0	1.0
Drive	X	0.285	-0.744	0.739
	Y	0.008	-22.27	0.103
	Z	0.242	5.98	0.260
Compliant	X	0.352	8.23	0.439
	Y	0.012	-19.4	0.182
	Z	0.146	5.870	0.330

Conclusion

The goal of this study was to determine if there were statistically significant differences in the global response of the GOBLET when it was tested using two different sets of control DOFs. In addition, we examined how a test engineer might judge the quality of a test at different levels using a several error metrics. Overall, combining visual and numerical assessments, it is difficult to tell which control configuration performs better. Visual assessment might lead one to the conclusion that the drive configuration performed better, but numerical assessment at different levels showed mixed results. At the total aggregate level, the dB error and G_{RMS} would suggest the compliant control performed better than the drive, but the PSDPM would suggest otherwise and visual inspection suggests they were similar. At the next level, the sum of each direction, the compliant configuration also appeared to perform closer to the field in all error metrics. The individual channel assessment appears that the drive configuration performed better than the compliant due to its lower dB error, especially in the X-direction and higher PSDPM values.

Overall, we learn that at different levels, visual inspection and error metrics did not give a clear picture of which control configuration performs "better." This conclusion shows that aggregate assessment techniques do not necessarily provide similar answers when comparing data at different levels of fidelity, showing that there is need to make a full assessment of each response. The importance of metric choice also cannot be overstated, with several of the metrics in this paper often showing disagreement. The disagreement between metrics highlights that metrics are application specific and should be used with intention. While we were not able to conclusively determine which control configuration performed the best, this study highlights the need for exercising skepticism when analyzing aggregate ASD response and for assessing the error in response using multiple, relevant techniques to get a clearer picture of what the data are showing.

Acknowledgments This study was funded by the Los Alamos Delivery Environments Program. This work has been reviewed for public release (LA-UR-24-30418).

References

1. Daborn, P. *Smarter Dynamic Testing of Critical Structures*. PhD thesis, University of Bristol, 2014.
2. Rohe, D.P., Nelson, G.D., and Schultz, R.A. "Strategies for shaker placement for impedance-matched multi-axis testing". In Walber, C., Walter, P., and Seidlitz, S., editors, *Sensors and Instrumentation, Aircraft/Aerospace, Energy Harvesting & Dynamic Environments Testing, Volume 7*, pages 195–212, Cham, "February" 2020. Springer International Publishing.
3. Cross, K., Melendez, G., and Zwink, B. "Natural excitation within a test frame experimental results.". *Proceedings of the 41st International Modal Analysis Conference*, February 2023.
4. Smallwood, D.O. and Gregory, D.L. "Evaluation of a six-dof electrodynamic shaker system.". Technical report, Sandia National Lab.(SNL-NM), Albuquerque, NM (United States), 2008.
5. Kramer, H., Schultze, J., Danforth, S., and Mann, B. "Quantifying differences between mimo and siso testing on the marc structure". In *Proceedings of the 42nd International Modal Analysis Conference*, February 2024.
6. Danforth, S., Johnson, S., Fenstermacher, K., Ramirez, A., Sedillo, H., Schultze, J., and Ferguson, E. "Developing methods for single-axis base excitation vibration testing with additional distributed shakers". In *31st International Conference on Noise and Vibration*, September 2024.
7. Lee, D., Ahn, T.S., and Kim, H.S. "A metric on the similarity between two frequency response functions". *Journal of Sound and Vibration*, 436:32–45, September 2018.